

## Supplemental Figure Legends

**Figure S1, related to Figure 1.  $\beta$ -Klotho is expressed in multiple cell types in the hypothalamus.**

(A) Generation of *Klb*-CRE mice.

(B) Southern blot analysis verifying targeting of 3' end of *Klb*-CRE mice.

(C-D) Immunofluorescence imaging of tdTomato in the (C) liver and (D) ventromedial nucleus (VMH) and arcuate nucleus (ARC) of the hypothalamus (top), and the area postrema (AP) and nucleus tractus solitarius (NTS) of the hindbrain (bottom) of *Klb*-CRE mice.

(E-F) Immunofluorescence imaging of the AP/NTS (E) and the nucleus accumbens (NAc) (F) of *Klb*-CRE;Ai14 tdTomato mice.

(G) FACS sorting in isolated hypothalami of WT and *Klb*-CRE;Ai14 tdTomato mice.

(H) Violin plots and percent abundance of hypothalamus cellular populations in *Klb*-CRE;Ai14 tdTomato mice identified by single cell RNA sequencing (scRNAseq) using 10X Chromium scRNAseq. UMI, unique molecular identifier. Scale bars, 100  $\mu$ m.

**Figure S2, related to Figure 2. FGF21 signaling to glutamatergic neurons is necessary and sufficient for FGF21-mediated sugar suppression.**

(A) Immunofluorescence imaging of tdTomato expression in Vglut2- (*Vglut2*-Cre;tdTomato), Vgat- (*Vgat*-Cre;tdTomato), and DAT- (*DAT*-Cre;tdTomato) expressing cells.

(B) Daily measurements of sucrose intake, water intake, and sucrose preference during two-bottle choice of 10% sucrose versus water in 11-13 week old male wild-type (WT) mice or mice lacking KLB in Vglut2-expressing cells (KLB *Vglut2*-KO), while receiving daily injections of vehicle (3 days) followed by daily injections of FGF21 (1 mg/kg; 3 days) via i.p. injection ( $n = 12-21$ /group).

(C) Fluid intake during two-bottle choice of 10% sucrose versus water in 11-13-week-old female WT or female KLB *Vglut2*-KO mice while receiving daily injections of vehicle (3 days) followed by daily injections of FGF21 (1 mg/kg; 3 days) via i.p. injection ( $n = 13-14/\text{group}$ ).

(D) Fluid intake during two-bottle choice of 10% sucrose versus water in 11-13-week-old male and female WT mice while receiving daily injections of vehicle (3 days) followed by daily injections of FGF21 (1 mg/kg; 3 days) via i.p. injection ( $n = 9-10/\text{group}$ ).

(E) Immunofluorescence imaging in the ventromedial hypothalamus (VMH) of WT mice, *Klb*-CRE;FL-hM3Dq mice, *Vglut2*-FLP;FL-hM3Dq mice, and *Klb*-CRE;*Vglut2*-FLP;FL-hM3Dq mice. Values are mean  $\pm$  SEM. (\*,  $P < 0.05$  compared to WT). Statistical analyses were conducted using 2-way ANOVA for multiple comparisons. Scale bars, 100  $\mu\text{m}$ .

**Figure S3, related to Figure 3. FGF21 does not signal directly to CRH- or Phox2b-expressing cells to suppress sugar intake.**

(A-B) Fluid intake during two-bottle choice of 10% sucrose versus water in 11-13 week old male WT mice or mice lacking (A) corticotrophin-releasing hormone- (KLB CRH-KO) or (B) paired-like homeobox 2b-expressing cells (KLB *Phox2b*-KO) treated with vehicle or FGF21 (1 mg/kg) i.p. injection for 3 days ( $n = 7-10/\text{group}$ ). Values are mean  $\pm$  SEM. (\*,  $P < 0.05$  compared to WT). Statistical analyses were conducted using 2-way ANOVA for multiple comparisons. Scale bars, 100  $\mu\text{m}$ .

**Figure S4, related to Figure 4. FGF21 signaling to the ventromedial hypothalamus (VMH) is not required to increase energy expenditure.**

(A) Fluorescence in situ hybridization (FISH) demonstrating co-localization of SF1 (green) and tdTomato (red) in the VMH of *Klb*-CRE;Ai14 tdTomato male mice.

(B) Violin plots of *in silico* analysis of *Klb* (left panel) and *Slc17a6* (*Vglut2*, right panel) mRNA transcript expression in KLB<sup>+</sup> VMH neurons using single-cell RNA sequencing (SMART-seq) data originally reported by Kim et al., 2019. The identity groups listed along the x-axis indicate identified subclusters of KLB<sup>+</sup> VMH neurons based upon differential gene expression analysis within KLB<sup>+</sup> expressing VMH neurons.

(C) Relative mRNA levels of the thermogenic genes *Bmp8b*, *Ucp1*, and *Elovl3* in brown adipose tissue (BAT) of 16-18-week-old, diet-induced obese (DIO) wild-type (WT) and mice lacking KLB in SF1-expressing cells (KLB SF1-KO) administered vehicle or FGF21 via osmotic minipump for 2 weeks (1 mg/kg/d) ( $n = 6-8$ /group).

(D-E) Plasma triglycerides (D) and food intake (E) in DIO WT and DIO KLB SF1-KO mice receiving continuous administration of vehicle or FGF21 via osmotic minipump for 2 weeks (1 mg/kg/d) ( $n = 6-8$ /group).

(F) Plasma glucose levels in WT or KLB SF1-KO mice receiving vehicle or FGF21 during an insulin tolerance test ( $n = 5-6$ /group).

(G) Area under the curve (AUC) for mice in (F). Values are mean  $\pm$  SEM. (\*,  $P < 0.05$  compared to WT). Statistical analyses were conducted using 2-way ANOVA multiple comparisons.

**Figure S5, related to Figure 5. FGF21 does not alter current-voltage relationship in KLB<sup>+</sup> VMH neurons.**

(A) Representative traces of membrane current steps applied to KLB<sup>+</sup> VMH neurons in vehicle and FGF21 injected (1 mg/kg, i.p.) mice to generate the current-voltage (I-V) plots.

**(B)** Plotting of the I-V relationship in KLB<sup>+</sup> VMH neurons in mice injected with vehicle or FGF21.  $n = 37$  neurons for both conditions from 4 mice.

**(C)** Plotting of the I-V relationship in KLB<sup>+</sup> VMH neurons in slices where FGF21 was bath applied directly to the slice.  $n = 15$  neurons for FGF21 added and 14 for aCSF from 3 mice each. Values are mean  $\pm$  SEM. Comparisons were made using a 2-way ANOVA w/ Sidak's multiple comparisons test.

**Figure S6, related to Figure 1. KLB<sup>+</sup> neurons are located in the anterior piriform complex.**

Fluorescence imaging for tdTomato positive cells in the Anterior Piriform Complex (APC) of 12-week old *Klb*-CRE mice following infection with a PHP.eb-FLEX-tdTomato virus.

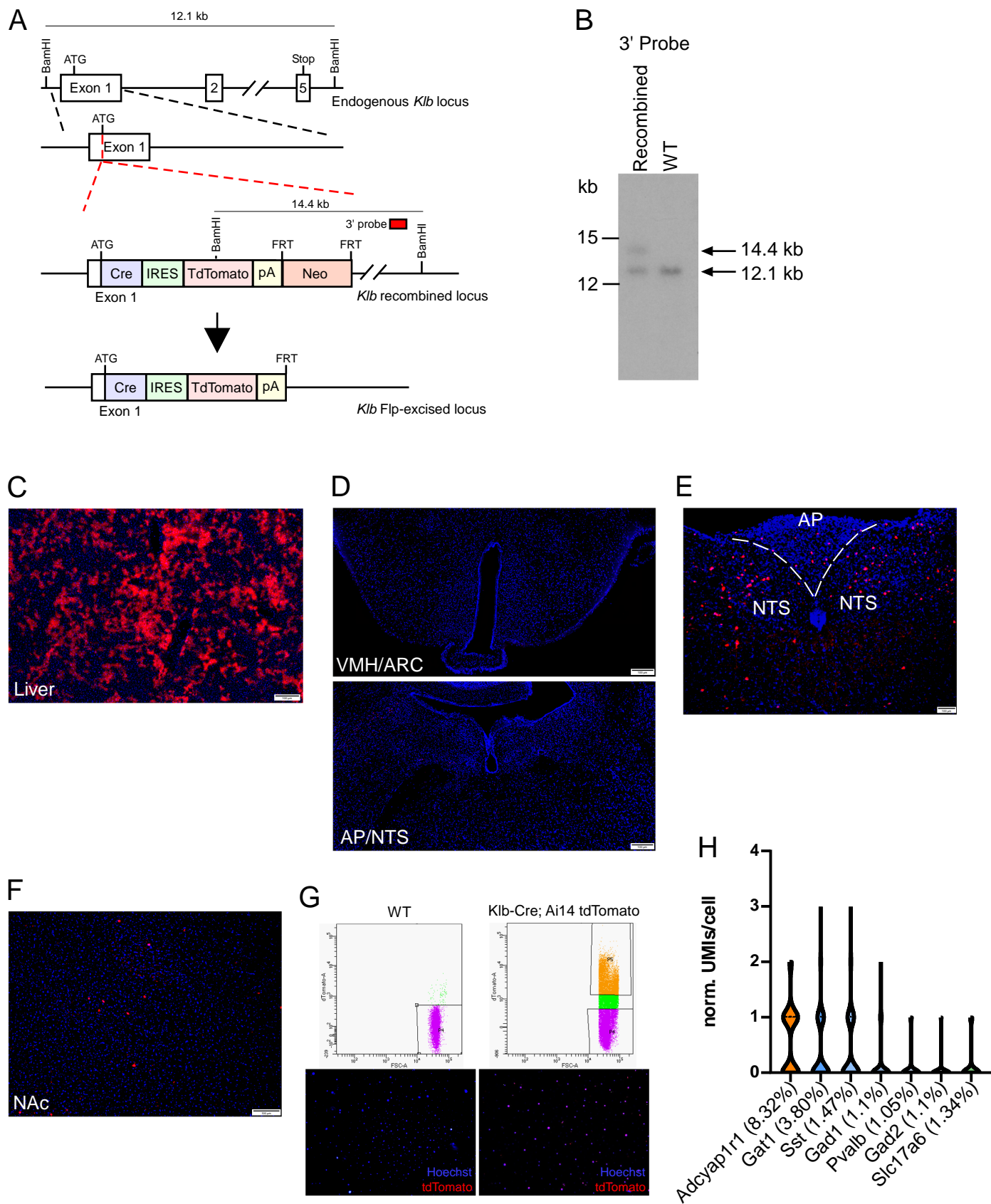


Fig. S1

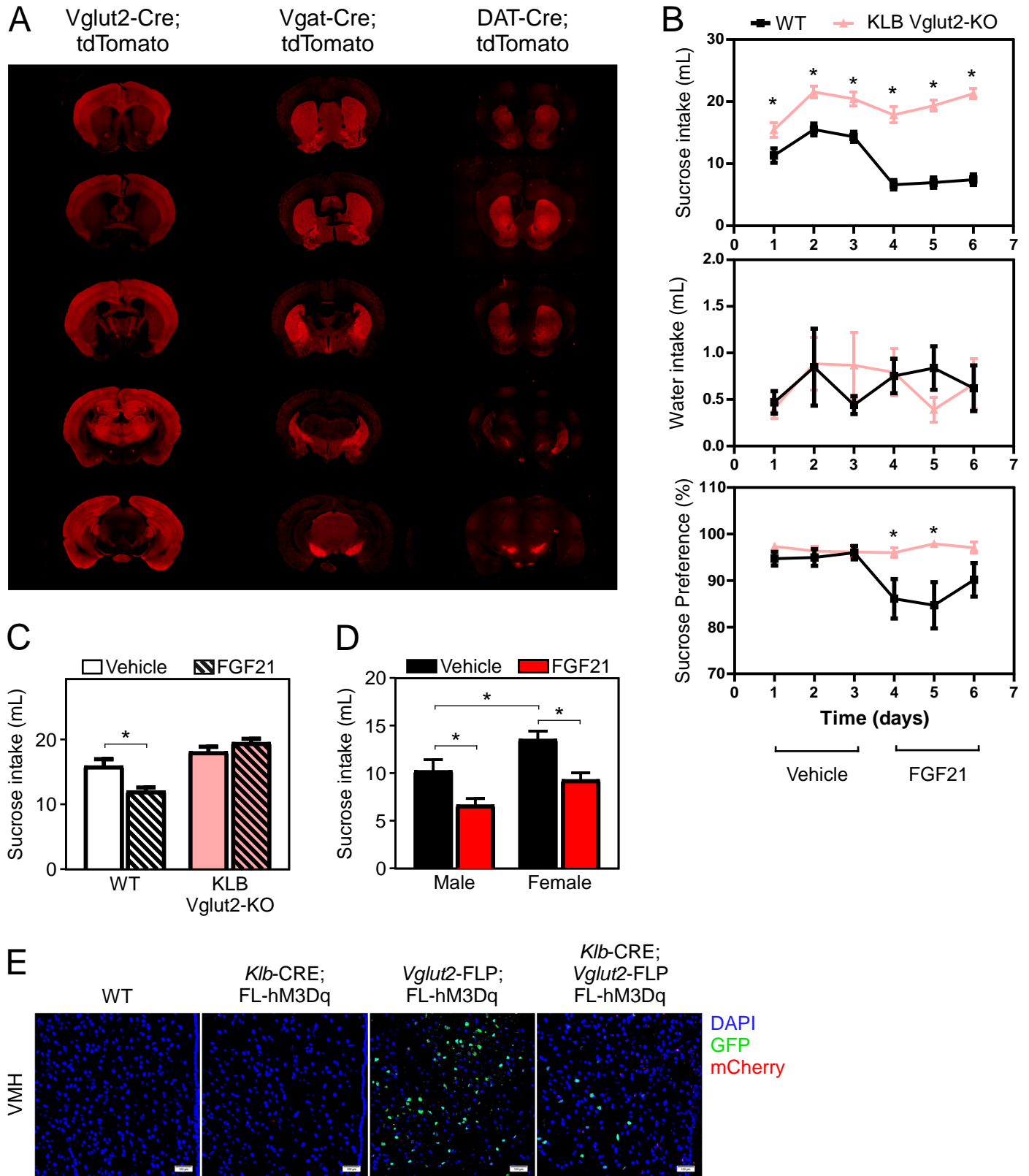


Fig. S2

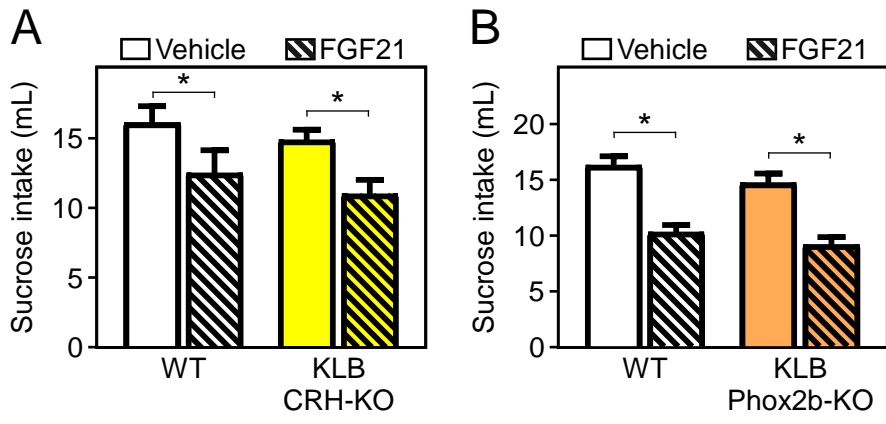


Fig. S3

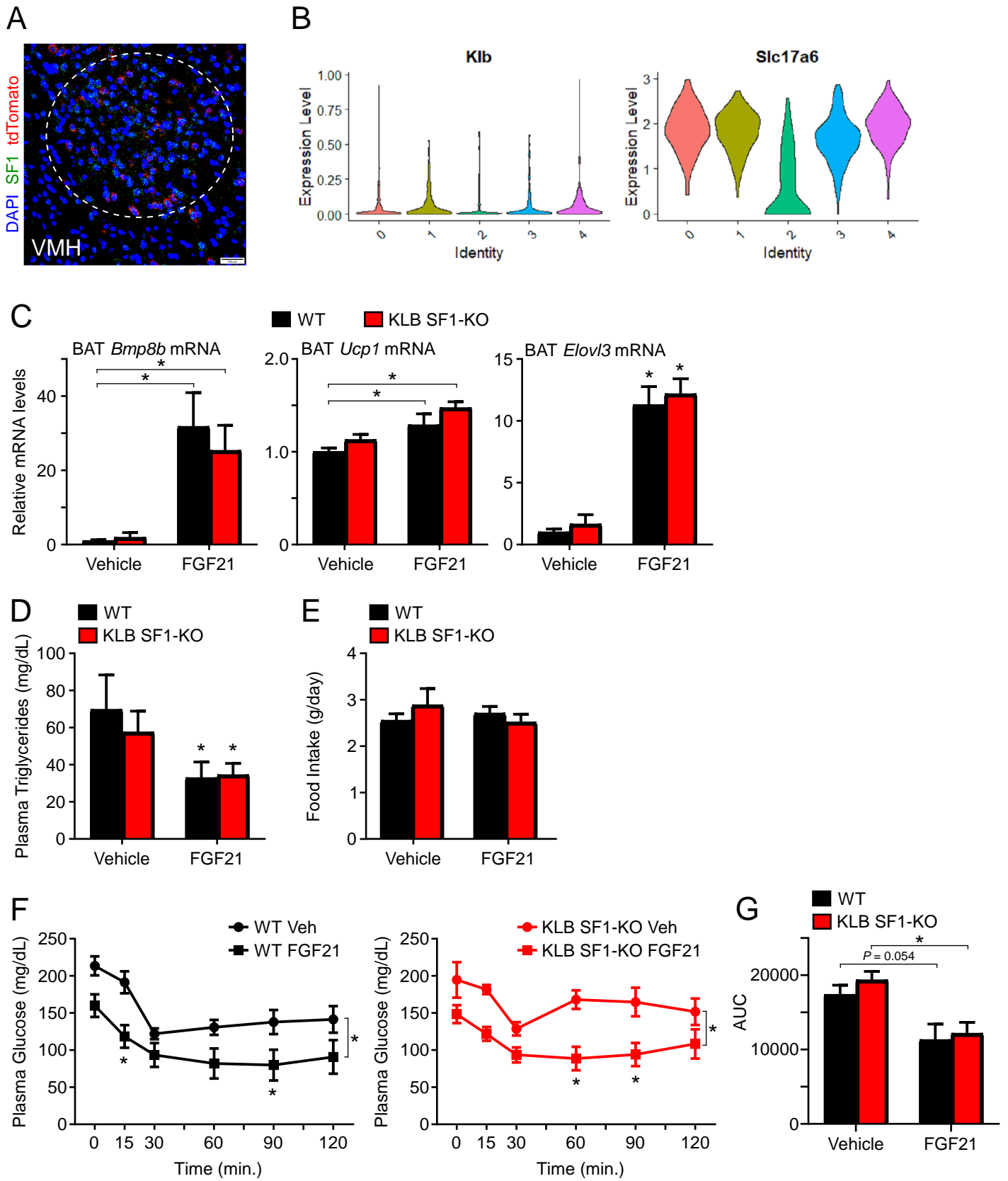


Fig. S4



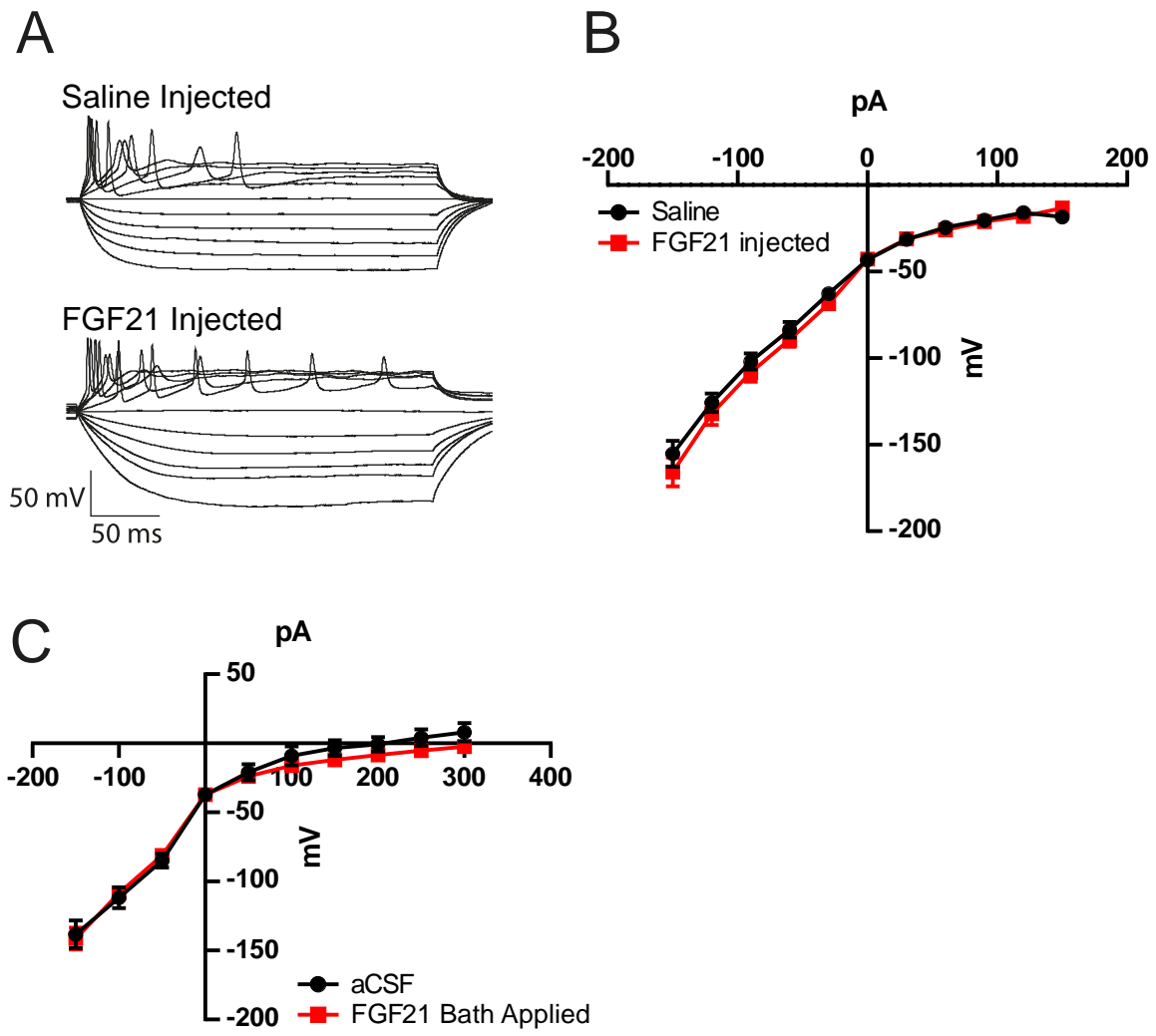


Fig. S5

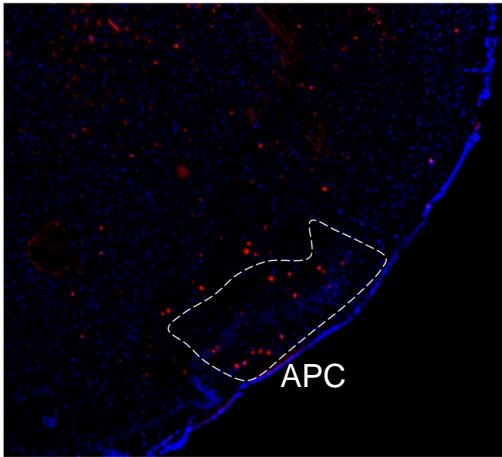


Fig. S6